Post Flight Report of Free Flight Test of Hayabusa-Type Larger Sample Return Capsule using Scientific Balloon in Australia

By Kazuhiko YAMADA[1)], Ryosuke ONO[2)], Yuma YAGI[1)], Tatsuro NAKAO[2)], Hiroki TAKAYANAGI[2)], Ryo SUGIMOTO[1)], Sota KUBOTA[3)], Hideyuki MORI[1)]

[1)] *Institute of Space and Astronautical Science, JAXA, Sagamihara, Japan*
[2)] *Research and Development Directorate, JAXA Sagamihara, Japan*
[3)] *Graduate School of Advanced Engineering, Tokyo University of Science, Japan, Tokyo, Japan*

Sample Return Capsule (SRC) is an important technology supporting deep space sample return missions. In particular, "Hayabusa" SRC is a globally remarkable technology that enables a direct re-entry from an interplanetary orbit. However, future more advanced sample return missions will also require the maturity and evolution of SRC technology, for example, a larger SRC. Therefore, in this study, a free flight test of Hayabusa-type larger SRC was carried out using a scientific balloon in Australia at May, 2023, in order to understand the aerodynamic characteristic and the attitude motion in transonic and subsonic regime and to demonstrate the free deployment of a parachute developed for the larger SRC. For this test, a larger Hayabusa-type experimental SRC, which has a diameter of 60cm and a mass of 45kg was developed. This test demonstrated that the experimental SRC flied without severe divergence of the attitude motion from a transonic region to a subsonic region and deployed a subsonic parachute successfully. Much valuable flight data, including the descent trajectory, the attitude motion and the parachute behavior in the deployment, were obtained. According to these data, the flight trajectory can be reconstructed by a numerical simulation and the validity of the design model for the parachute deployment shock load is confirmed, compared with the empirical database.

Key Words: Hayabusa-type sample return capsule, Aerodynamic stability, Parachute, Balloon experiment

1. Introduction

"Hayabusa" mission, which is the first successful sample return mission from an asteroid in world, give a strong impact and a drastic innovation for a planetary exploration field[1)]. The scientific significance and value obtained by bringing celestial samples from deep space back to Earth for the detail analysis with huge and powerful analyzers on the ground was demonstrated. Due to this achievement, sample return missions from small celestial bodies become one of the core pillars in the planetary exploration field. "Hayabusa 2" mission[2)] in Japan (launch in 2014, return in 2020) and "OSIRIS-REx" mission[3)] in U.S. (launch in 2016, return in 2023) was carried out, following "Hayabusa" mission. Furthermore, in Japan, Mars Moon Exploration (MMX) mission[4)] including the sample return from Phobos is being prepared for a launch in 2026 and some discussions on the sample return from deeper space, like Jovian and Saturn's sphere, also started. Globally, NASA's New Frontiers Program 5, which is a large-scale competitive program, lists the sample return mission from comets as one of its key targets[5)]. One of the important and essential technologies to realize and support those future sample return missions is Sample Return Capsule (SRC) technology. Among them, the SRC of Hayabusa, which realizes the world's first sample return from an asteroid in the Hayabusa mission, is globally remarkable, because it has the capability to achieve the direct Earth re-entry at 12 km/s (the world's highest class) from an interplanetary orbit, which is a rare technology in the world. Additionally, its size is 40 cm in diameter and 16 kg in total reentry mass. It is one of the smallest in the world.

For realizing future advanced sample return missions in future, the enhancement in SRC technology is also indispensable. Scientists demand samples from more distant celestial bodies and/or a larger amount of samples for higher scientific results, like an investigation of the origin of the solar system and life. In order to return from more distant celestial bodies, an SRC that can enter the Earth's atmosphere at higher speeds is required. And in order to return a larger amount of samples, a larger SRC is needed. SRC technology must continue to evolve to satisfy these requirements. Therefore, in this study, a free-flight test of a larger sample return capsule based on the "Hayabusa" SRC was conducted using a scientific balloon, as part of the development of a larger Hayabusa-type SRC. The objectives of this flight test are to acquire flight data related to the following two technical issues, which are difficult to verify in ground tests, under free-flight environment and completely the same conditions as the actual flight.

(1) Aerodynamic behavior in the transonic to subsonic regime in free flight conditions to understand the aerodynamic instability.
(2) Parachute behavior during parachute deployment process to verify the design model for opening shock load.

For this flight test, the experimental SRC, which is equivalent shape and size to the SRC for MMX, was developed, and this flight test of this experimental SRC was conducted in May 2023 in Alice Springs, Australia. In this paper, the experimental SRC, the flight test system, the flight operation at the site, obtained flight data, and the results and the considerations of the post flight analysis were described.

2. Experimental method

2.1 Experimental vehicle

In this study, the flight test for a larger Hayabusa-type sample return capsule was carried out. Figure 1 shows an external drawing of the experimental SRC with dimensions. The external and aerodynamic shape is similar to that of the Hayabusa SRC, with a diameter of approximately 60cm (the actual diameter is 59.1cm because the edge was shaved to fix by Marman cramp). The aerodynamic shape is completely identical to that of MMX-SRC.

Figure 2 shows a CAD model of the experimental SRC. Like the Hayabusa SRC, the instrument module is sandwiched between the front and back heatshield. In the actual SRC, the sample container is equipped in the center of the instrument module, but in this experimental SRC, onboard avionics, including batteries, telemetry system, recovery support devices and sensors are equipped in this part. And the GPS and Iridium antennas are attached above and below the instrument module to identify its location for recovery. Cross-type canopy is adopted for the parachute. The parachute is packed in slender cylinder bag and is stored around the instrument box. The parachute is ejected and deployed by drawn with the back heat shield at the same time as a jettison of the front and back heat shields by the pyrotechnics. The concept of the parachute system is common to the Hayabusa/Hayabusa2 SRC and MMX-SRC. The parachute storage space and shape of the experimental SRC is completely the same as that of MMX-SRC. Both the front and back heat shields are a dummy made of general plastic, but its mass is the same as that of the MMX-SRC. On the front heat shield, a heatshield jettison and parachute ejection mechanism (pyrotechnics) and a sensor board for measuring pressure on the front side are mounted. 5 pressure ports including stagnation point are placed on the front surface of the front heat shield. On the back heat shield, tiny hooks are attached on the inner side to connect to the storage bag for drawing a parachute

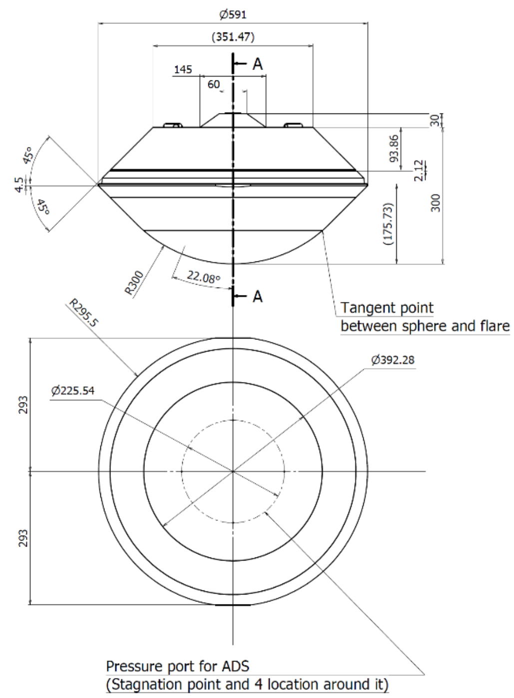

Fig. 1. Drawing of the SRC experimental vehicle (dimensions: mm)

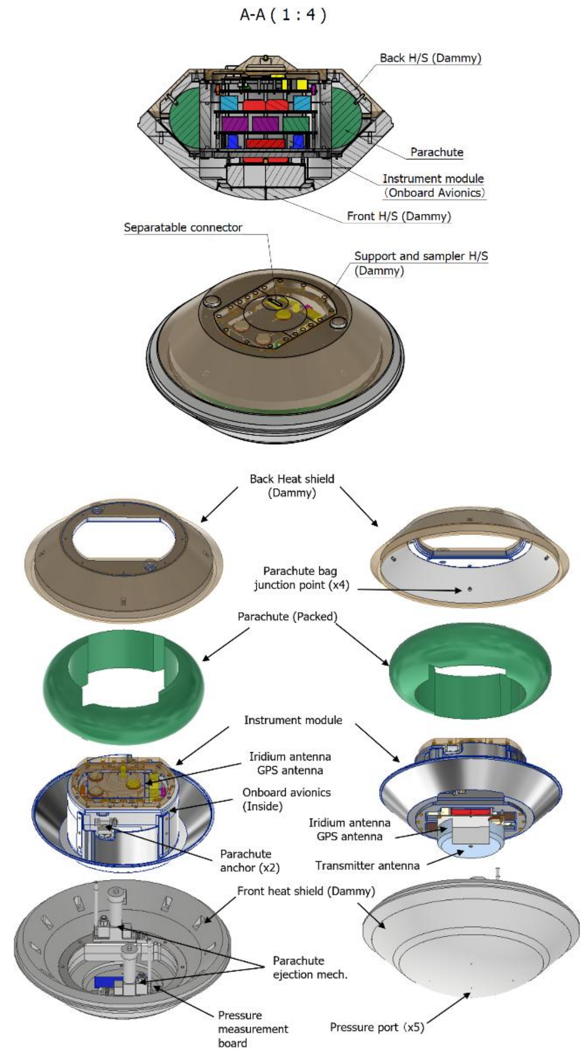

Fig. 2. Cross section view(upper), bird's-eye view(middle) and exploded view (bottom) of CAD model of the SRC experimental vehicle

Figure 3 shows an external view of the experiment SRC for the flight test. It is a Hayabusa-type capsule with a diameter of 60 cm, and its aerodynamic (external) shape dimensions are as shown in Figure 1. The total mass of the experimental SRC is 45.4 kg. The center of gravity is located 163.6 mm behind the stagnation point of the front heat shield on the axisymmetric body axis. This corresponds to 54.5% position when the total length is 300 mm, and this is the same as the one of the Hayabusa2 SRC. The offset of the center of gravity from the body axis is less than 1 mm and it is about 0.15 mm according to the estimation based on CAD model. This value is less than the measurement accuracy, and it can be considered that the center of gravity of the experimental SRC is almost on the body axis. The center of gravity and moment of inertia were calculated by summing the mass of each component and parts on the CAD model. The mass of each component and parts on the CAD model were adjusted, compared with the actual measured values. In order to verify the estimated values, a single point suspension test was conducted for the center of gravity position, and a pendulum test was conducted for the moment of inertia. It is confirmed that the values estimated from the CAD model are within the measurement accuracy of those simple actual measurement tests. The major specifications of the experimental SRC, including mass property, are listed in Table 1.

Fig. 3. Photo of the experimental SRC for the flight test

Table 1. Major specification of the SRC experimental vehicle

Specification items	Value
SRC total mass	45.4kg
Position of the center of gravity from stagnation of front H/S	163.6mm (estimated from CAD model)
Offset of the center of gravity from body axis	0.155mm (estimated from CAD model)
Moment of inertia around the body axis	1.327kgm^2 (estimated from CAD model)
Moment of inertia around the perpendicular axis to body axis.	0.871~0.878kgm^2 (estimated from CAD model)
Mass of instrument module (including parachute)	21.8kg
Designed drag area of parachute	6.4m^2
Mass of front H/S	18.3kg
Mass of back H/S	5.3kg
Time of trigger for parachute deployment from SRC separation	115sec

The major measurement items and sensors in this flight test are listed in Table 2. While a part of the obtained flight data is transmitted to the ground station via the telemetry system during the flight, most of the flight data is recorded in the onboard memory in instrument module and retrieved after the recovery. The sampling rate described in Table 2 is the rate of recording to the onboard memory.

Table 2. Major measurement items and onboard sensors.

Measurement items	Sensor (Model) : Sampling rate
Position	GPS (Firefly) : 10Hz
Attitude and motion	Inertial sensor (MTi-1-8A7G6):100Hz
Attitude against flow	Pressure sensor: 10Hz (SSCDRNN015PAAA5 at stagnation) (SSCDRRN001PDAAS around stagnation) (4525-SS5B015AP at backside)
Backside view (Movie)	Action Camera (SJ4000):60Hz
Shock load	Acceleration logger (MSR 165) : 1600Hz

2.2 Flight test sequence

This flight test using a scientific balloon was conducted in the sequence shown below.

1) A balloon with a gondola carrying the experimental SRC ascend to the required altitude (about 40 km).
2) After reaching the required altitude and the droppable area, the health check of the experimental SRC and the drop preparation sequence is executed.
3) The experimental SRC is separated by the command from the ground station and the flight test is started. A gondola-mounted camera captures images of the experimental SRC just after separation.
4) The experimental SRC accelerates in free descent, to the transonic regime, where Mach number is more than 1.0.
5) The behavior of the experimental SRC, including the motion and attitude, is measured during the free flight. These flight data are recorded in the onboard memory.
6) The heat shield jettison and the parachute deployment are automatically executed by a timer sequence in 115 seconds after the SRC separation at an altitude of about 13km.
7) The instrument module makes a slow descent with the parachute and a soft landing at a speed of about 7m/s.
8) After the landing, the landing position of the instrument module obtained by GPS is transmitted via Iridium satellite network to the recovery team.
9) The instrument module, the front heat shield and the back heat shield of the experimental SRC and the gondola are recovered.

In this flight test, the experimental SRC jettisons the front and back heat shields during the descent. Hence, three objects, that are the instrument module with the parachute, the front heat shield and the back heat shield landed. Figure 4 shows a schematic image of the flight test sequence.

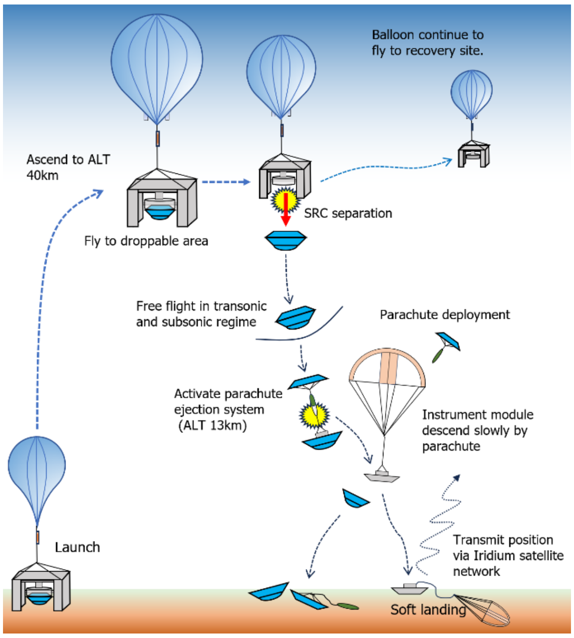

Fig. 4. Schematic image of the flight test sequence

3. Flight operation

The flight test was conducted on May 11, 2023, in Alice Springs, Australia. The Scientific balloon B23-02 with a volume of 300,000 m^3 was launched early in the morning at 7:39 local time for this test. Figure 5 shows the balloon and gondola just prior to launch. The experiment SRC was mounted on the bottom of the gondola which was hung from the crane.

Fig. 5. Photo of the scientific balloon B23-02 and gondola just before launch in Alice Springs, Australia,

After the balloon was released, it ascended steadily and flew almost east due to the jet stream and westerly wind at the stratosphere. At around 11:25 a.m. (local time), when the balloon entered the droppable area, which is located about 200 km east of the launch site, the operation for the separation of the experimental SRC from gondola was executed and the free-flight test was started.

The experimental SRC separated from the gondola accelerated to transonic speed, where is at Mach number of more than 1.0, in the free descent and the parachute was deployed at about 115 seconds after the SRC separation as designated. After the parachute deployment, the instrument module made a slow descent and a soft landing approximately 1400 seconds after the separation. Figure 6 shows snapshots taken by gondola-mounted and SRC onboard cameras. The two images on the left show the experimental SRC just after separation from the gondola and it can be confirmed that the experimental SRC was separated quietly in a stable attitude. The image in upper right is a balloon and gondola captured from the experimental SRC immediately after the separation, and the lower right image is the deployed parachute during a slow descent. According to these images, the normal dropping from the gondola, the free flight without severe divergence of the attitude motion, and the successful deployment of the parachute were confirmed.

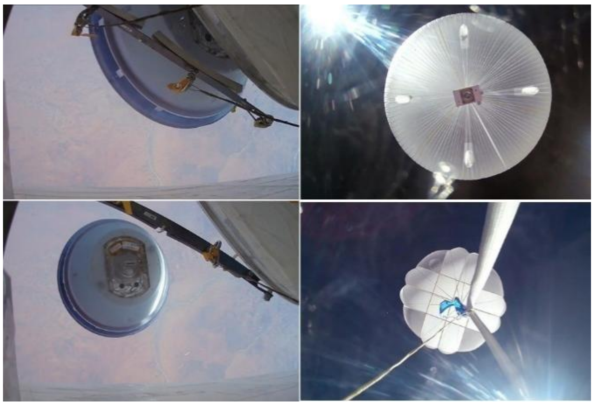

Fig. 6. Snapshots captured with gondola-mounted cameras, and SRC onboard cameras. (left: Experimental SRC captured by gondola mounted cameras just after separation, right upper: balloon and gondola captured by SRC onboard camera just after separation, right lower: deployed parachute captured by SRC onboard camera)

On the other hand, after the experimental SRC was separated, the balloon continued to fly eastward and was guided to a suitable location for the recovery. At 2:35 p.m. (local time), a gondola separation command was sent for the flight termination. The gondola landed about 40 minutes after separation and the balloon's flight was finished.

As for the recovery of the experimental SRC, a small aircraft was flown immediately after the landing of the experimental SRC to the landing point of the instrument module indicated by the GPS & Iridium positioning system and can find the instrument module from above. The instrument module was then recovered by a helicopter the next day. Also, regarding the heat shields, both front and back heat shields were able to be found and recovered before the end of the day, searching surroundings around the landing point of the instrument module, based on the predicted descent trajectory. And all flight data to be recorded inside the instrument module was successfully retrieved. Figure 7 shows the instrument module, the parachute and the heat shields found during the recovery operation.

Fig. 7. Photos of the parachute (left upper), the instrument module (left lower), the back heat shield (right upper) and the front heat shield (right lower), at recovery.

4. Reconstruct of flight trajectory

As a first step of the flight data analysis, the flight trajectory was reconstructed and the flight environments and the aerodynamic performance of the experimental SRC in the free flight were estimated. In this section, the altitude history obtained by GPS was reproduced in the simulation by adjusting the input parameters for the descent trajectory simulation. In this trajectory simulation, the motion of a point mass in 3-dimensional space was solved, considering only the aerodynamic drag force and the gravity force. The parameters assumed for the trajectory simulation are summarized in Table 3. The values listed in Table 3 are values adjusted to reproduce the altitude history obtained by GPS.

The mass of the whole experimental SRC and the instrument module are measured values. For the separation time, position, and initial horizontal velocity, the values in the actual flight were used. The atmospheric model was estimated from the global forecast data closest to the flight time. Under those conditions, the SRC's drag coefficient, the parachute drag area, and the parachute deployment time were adjusted to correspond to the GPS altitude history and the simulation results.

The results are shown in Figure 8. X time on the horizontal axis indicates the elapsed time since the experimental SRC was separated from the gondola. According to the flight data, the experimental SRC was separated at an altitude of 39.64 km, dropped in free-fall, and accelerated to a maximum speed of 365 m/s. After that, it decelerated by the aerodynamic force and deployed the parachute at an altitude of 13.4km and a speed of 142 m/s. After the parachute deployment, the experimental SRC made a slow descent and a soft landing at a descent speed of 7.3 m/s at 1413 seconds after the separation. And the result of the trajectory simulation with adjusted parameters faithfully reproduces the flight data. The result suggests that the SRC's drag coefficient was on average, about 80% of the aerodynamic database at zero angle of attack. It is considered that the reduction of the drag coefficient is caused by an attitude oscillation of the experimental SRC. And the drag area during the slow parachute descent was somewhat larger than the design value of the parachute canopy.

Table 3. Parameter list of the post flight simulation for reconstruction of flight trajectory

Parameter	value
SRC total mass	45.4kg
SRC diameter (reference area)	0.6m (0.283m^2)
SRC drag coefficient	0.8 times as Hayabusa database in zero angle of attack[7]
Instrument module mass including parachute	21.8kg
Drag area of parachute	6.8m^2 (designate drag area : 6.4m^2)
Time of parachute deployment from SRC separation	115.7sec
Atmospheric model (density and wind profile)	Global forecast data provided by NCEP at 2023/5/11 0:00(UT)
Time of SRC separation	2023/05/11 01:55:50(UT)
Altitude at separation	39.64km
Location at separation (Latitude, Longitude)	(S 23.5802, E136.22512)
Horizontal velocity at separation	19.34m/s in the east direction 1.34m/s in the south direction

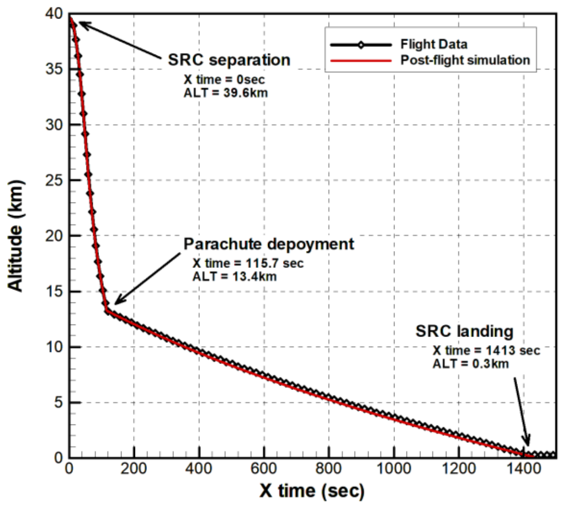

Fig. 8. Comparison of the altitude history between the flight data obtained by GPS and the simulation results with adjusted parameters.

Based on the results of this trajectory simulation, the aerodynamic environments were estimated. Figure 9 shows the time history of the dynamic pressure along the flight trajectory. From this result, it was estimated that the maximum dynamic pressure reached 2.85 kPa about 80 seconds after the SRC separation, and that the dynamic pressure at the parachute deployment was about 2.6 kPa. Figure 10 shows the time history of Mach number. The experimental SRC reached a maximum Mach number of 1.2 in 50 seconds after the separation, and it was confirmed that the transonic flight, which is an important objective of this test, was achieved. The SRC then decelerated to a Mach number of approximately 0.5 when the parachute deployed.

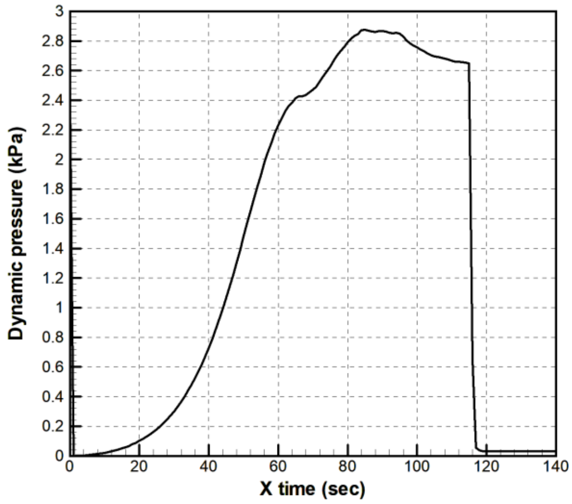

Fig. 9. Time history of the dynamic pressure estimated by the trajectory simulation with adjusted parameters

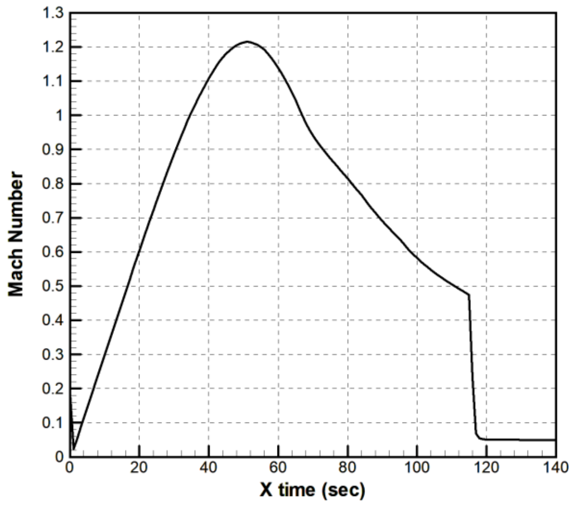

Fig. 10. Time history of Mach number estimated by the trajectory simulation with adjusted parameters

The Mach number can also be estimated from the air data sensors (ADS), which estimates the flow condition based on the pressure distribution on the front heat shield. The Mach number in flight test was estimated by comparing the pressure coefficient (C_M) with respect to the Mach number obtained by the following equation (1) with the results of the wind tunnel test. In equation (1), *Po* is the absolute pressure at the stagnation point, and ΔPn is the differential pressures between the pressures at pressure ports around the stagnation point and stagnation pressure.

$$C_M = \frac{\Delta P_1 + \Delta P_2 + \Delta P_3 + \Delta P_4}{4\, P_0} \quad (1)$$

A comparison of the Mach number histories estimated from the ADS and one estimated from the trajectory simulation is shown in Figure 11. The results estimated by ADS also suggest that the SRC was flying in the transonic region from around 40 seconds after the separation. However, it is difficult to estimate accurate values for the Mach number history estimated from the ADS because of the large temporal variation during the period from 40 to 80 seconds, when the experimental SRC was thought to be flying at transonic speed. This variability is probably related to the intense attitude motion of the experimental SRC during the transonic free flight. By eliminating the influence, the exact estimation of Mach number from ADS results is future work.

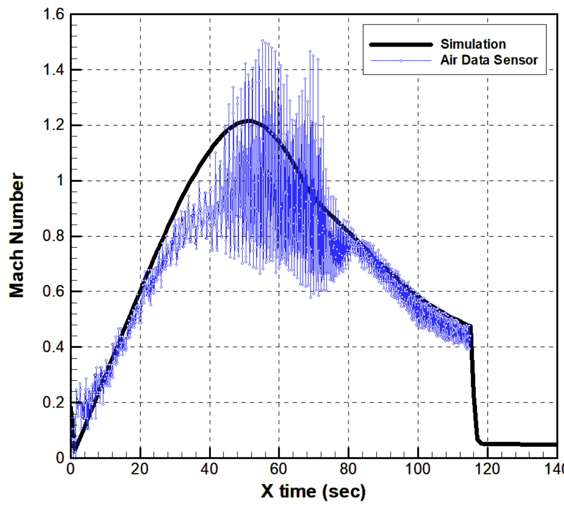

Fig. 11. Mach number history estimated using the air data sensor system.

5. Flight data analysis

5.1 Attitude motion

This section presents the flight data on the attitude motion of the experimental SRC during the free flight, which is one of the key objectives of this study. Figure 12 shows the 3-axis angular velocity history from the SRC separation to the parachute deployment, where the Z axis is the body's axisymmetric axis and the X and Y axes are perpendicular to it. The results show that after the experimental SRC was separated, the oscillating motion gently started around an axis perpendicular to the body axis. This oscillation developed rapidly in 35 seconds after the separation. Around 55 seconds after the separation, rotation around the body axis also started and the oscillation of the X and Y axes were interchanged with the amplitude increasing to 300 deg/s at 70 seconds after the separation. 35 seconds after the separation, when the oscillation started to develop rapidly, it had just exceeded Mach number 1.0 and reached the transonic region, as compared with the Mach number history in Figure 10. Therefore, this result indicates that the typical aerodynamic instability in the transonic region can be observed. The time when the increase of its amplitude stopped at 70 seconds after the separation, agrees with the end of the transonic flight. Thereafter, the experimental SRC flew to the parachute deployment without any divergence in its attitude motion, although the oscillations were slightly damped and continued to be about 250 deg/s in an amplitude. The period of this angular velocity oscillation was approximately 0.8 seconds (1.25 Hz). Based on this period and the maximum amplitude of the angular velocity (300 deg/s), the maximum attitude angle of the oscillation was estimated to be about ±38 degrees by assuming a sinusoidal oscillation.

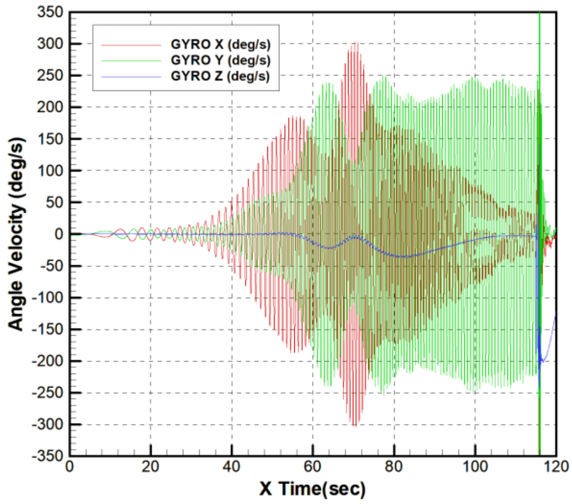

Fig. 12. 3-axis angle velocity history measured by the internal sensor, from the separation to the parachute deployment.

Next, the results of the estimation of the attitude against air flow from the ADS are presented. The angle of attack in the flight test was estimated by comparing the pressure coefficient (C_γ) with respect to the angle of attack obtained by the following equation (2) with the results of the wind tunnel test.

$$C_\gamma = \sqrt{{C_\alpha}^2 + {C_\beta}^2}, C_\alpha = \frac{\Delta P_1 - \Delta P_3}{P_0}, C_\beta = \frac{\Delta P_2 - \Delta P_4}{P_0} \quad (2)$$

Figure 13 shows the time history of an angle of attack around the axis perpendicular to the body axis, and Figure 14 shows the angular velocity history calculated by differentiating it. The angle of attack could not be estimated during the 20 seconds immediately after the separation because the sufficient differential pressure could not be measured to calculate the angle because of low atmospheric density and low speed. On the other hand, from 20 seconds after the separation until the parachute deployment, the time history of the angle of attack could be estimated from ADS. The result shows that, similar to the angular velocity sensor results in Figure 12, the attitude oscillation developed rapidly around 35 seconds, reached a maximum oscillation around 70 seconds and maintained its amplitude thereafter to the parachute deployment. Since the angle of attack can be obtained directly from the ADS, this result suggests that the amplitude of attitude oscillation may have reached up to 40 degrees. However, according to a comparison of the time history of the angular velocity estimated from ADS and the results obtained from the angular velocity sensor, the value obtained from the ADS sensor is about 10% larger than one of angular velocity sensor. It is also considered that intense attitude oscillation makes it difficult to estimate accurate values about attitude, as discussed in the Mach number estimation in the previous section. Improving the accuracy of attitude estimation by ADS will also be future work.

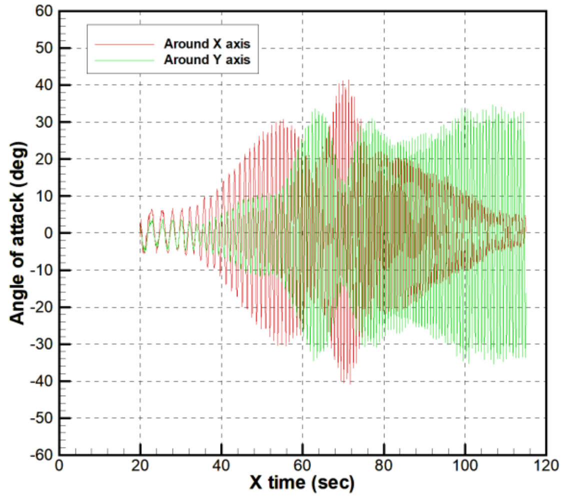

Fig. 13. Time history of the angle of attack around the X axis and Y axis estimated from the air data sensors (ADS).

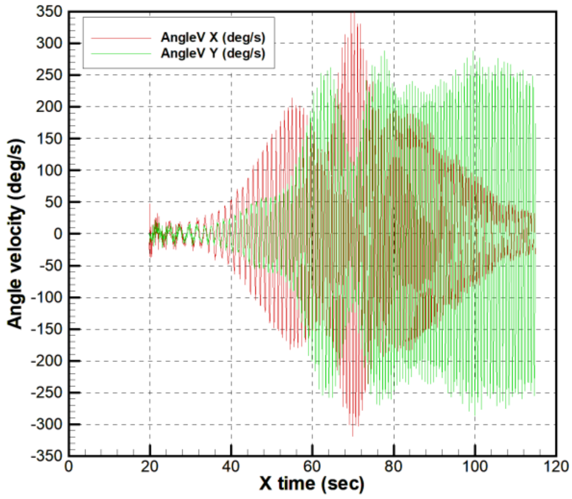

Fig. 14. Time history of the angle velocity around the perpendicular axis to body axis obtained by differentiating the angle history estimated from the air data sensors (ADS).

5.2 Parachute deployment

Observation and measurement of the parachute deployment behavior is another important objective in this study. Figure 15 shows sequential images at the parachute deployment captured by the onboard camera mounted on the backside of the experimental SRC. These are snapshots between 0.13 and 1.13 seconds, with setting the time to activate the parachute deployment pyrotechnics as 0 seconds. The image at 0.13 seconds shows that the back heat shield was ejected as soon as the pyrotechnic device was activated. And the parachute bag and the suspension lines are in the image at 0.53 seconds and the parachute risers are in the image at 0.63 seconds. It is confirmed that the parachute was drawn out by the back heat shield by this timing. Then, the image at 0.73 seconds shows that the parachute was unpacked from the storage bag. The parachute was rapidly deployed between 0.93 and 1.03 seconds and was almost fully deployed at 1.13 seconds according to these images.

Fig. 15. Sequential images captured by the onboard camera during the parachute deployment at 0.1 second intervals.

Figure 16 shows the acceleration history in the body axis direction during parachute deployment as measured by a shock logger (MSR-165) with a high sampling rate (1600 Hz). Since two shock loggers were installed, both results for the two units are plotted in Figure 16. The time on the horizontal axis is set to 0 seconds when the acceleration related to the activation of the parachute deployment pyrotechnics was detected. According to comparison with the images in Figure 15, it is indicated that the spike-like impact between 0.6 and 0.7 seconds is associated with cutting the temporary threads of the storage bag when the suspension line or parachute riser is drawn out. Then, the acceleration increased as the parachute deployed, and the maximum load was measured at approximately the same time as the full deployment of the parachute, approximately one second after the activation of the pyrotechnics for the parachute deployment.

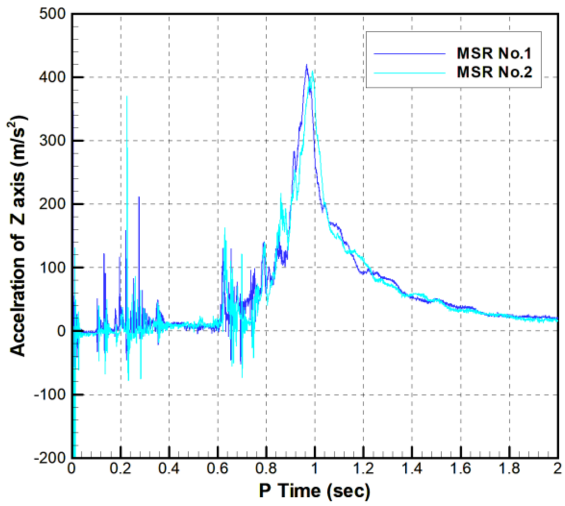

Fig. 16. Acceleration histories in the direction of the body axis during parachute deployment as measured by the two acceleration loggers (MSR 165)

From the impact load, the parachute opening load coefficient (Cx), which is important for the parachute design, can be estimated using the following equation (3).

$$C_x = \frac{m a_z}{q\, C_D S} \quad (3)$$

From the results in Figure 16, the maximum impact acceleration (a_z) is $420 m/s^2$. From the dynamic pressure history in Figure 9, the dynamic pressure (q) at parachute deployment is 2.65 kPa. The drag area of the parachute ($C_D S$) is set as a design value of the parachute canopy, which is $6.4 m^2$ and the mass of the instrument module (m) is 21.8kg. Under these conditions, the opening load coefficient (Cx) is calculated as 0.54.

A comparison of this result with the empirical model used to design the parachute is shown in Figure 17. In the design model, the opening load coefficient is expressed as a function of the Mass ratio (Rm), shown in the following equation (4). In the equation (4), the ρ is an uniform flow density, $C_D S$ is a drag area of the parachute canopy and Mt is the total mass of the experimental SRC including the parachute mass.

$$R_m = \frac{\rho\, (C_D S)^{1.5}}{m_t} \quad (4)$$

In Figure 17, two kinds of the empirical models are plotted. These are the maximum model and average model, which are described in Ref. 8) and Ref. 9), respectively. This comparison confirms that the opening loads observed in this flight test are close to the average empirical model.

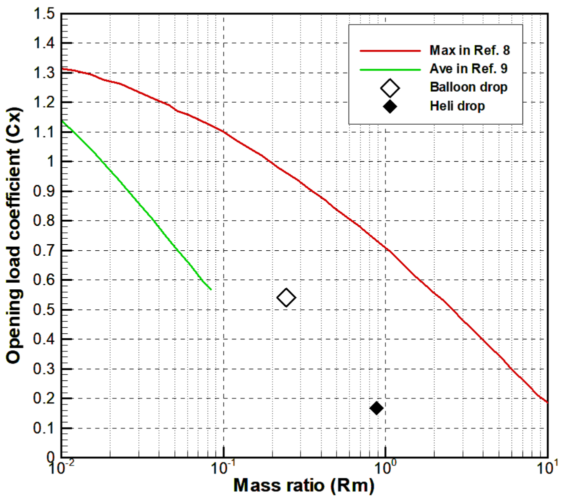

Fig. 17. Comparison of the empirical model used in the design and the flight data for the parachute opening load coefficient.

And, according to both design models, the opening load coefficient increases as the mass ratio decreases. Figure 17 also shows the flight data obtained in the past research when the parachute deployment tests were conducted at a low altitude by dropping from a helicopter using an experimental SRC and a parachute with the same specifications[10]. The result indicates that in the case of the combination of the SRC and the parachute used in this test, the relationship between the mass ratio and the opening load coefficient is in accordance with the same trend estimated from the empirical models. The results showed that a larger Hayabusa-type SRC and a cross-type parachute have a slightly higher opening load than the average model, but a sufficient margin from the maximum model.

6. Conclusions

Sample return capsule is one of the key technologies for advanced sample return missions in the future, and the maturation and evolution of the SRC technology is indispensable to realize it. In the near future, at least, a larger SRC will be requested in order to return a larger amount of sample. This balloon experiment described in this paper was planned as part of the development of a larger SRC. The larger Hayabusa-type experimental SRC, which is larger than the Hayabusa SRC, with a diameter of 60 cm and a mass of 45 kg, was dropped from an altitude of about 40 km using a scientific balloon to conduct a free-flight test from the transonic to subsonic regime. In this flight test, the attitude motion caused by the aerodynamic instability that develops in the transonic flight and continues until the subsonic speed was observed and measured. The attitude motion of the experimental SRC in this test did not diverge, but an intense oscillation was observed, with an amplitude of nearly 40 degrees. Additionally, in this test, the cross-type parachute was deployed successfully at high altitude and its behavior and opening shock loads can be measured. The flight data and knowledge obtained in this test are useful for the design of future SRCs with different sizes and mass properties, including larger sizes.

References

1) KAWAGUCHI J. “Mission to Asteroid Itokawa: The Hayabusa Project”, 14th Australian International Aerospace Congress, Key Note Address, 2010, Feb. 28-March 3, Melbourne. (2010)
2) Yuichi Tsuda, Makoto Yoshikawa, Masatoshi Hirabayashi and Shota Kikuchi, “Chapter 1 - Hayabusa2 as the beginning of deep space sample return”, Hayabusa2 Asteroid Sample Return Mission, 2022, P1-3
3) D.S Lauretta, at el. “OSIRIS-REx: Sample Return from Asteroid (101955) Bennu”, Space Science Reviews volume 212, pages 925–984 (2017)
4) K.Kuramoto, et. al. “Martian Moons Exploraton (MMX) conceptual study update” ,49th Lunar and Planetary Science Conference 2018 (LPI Contrib. No. 2083, 2143.pdf) (2018)
5) NASA, "DRAFT Announcement of Opportunity New Frontiers 5", NNH23ZDA006J, Release Date January 10,2023,
6) Yoshifumi Inatani and Nobuaki Ishii, “Design Overview of Asteroid Sample Return Capsule”, The institute of Space and Astronautical Science Report SP No.17, March 2003. Page 1-15
7) Koju Hiraki and Yoshifumi Inatani, "The Aerodynamic Data Base for Asteroid Sample Return Capsule", The institute of Space and Astronautical Science Report SP No.17, March 2003. Page 345-363
8) T. W. Knacke, “Parachute Recovery Systems Design Manual,” ADA247666, 1991.
9) E. G. Ewing, H. W. Bixby, T. W. Knacke, “Recovery Systems Design Guide ,” AFF DL TR 78 151 , 1978
10) Hiroki Takayanagi, Tatsuro Nakao, Ryosuke Ono, Takahiro Moriyoshi, Masahito Mizuno, Yasunori Nagata, and Kazuhiko Yamada, “Research and Development of Flight Measurement System for Free Flight Experiments”, Journal of Evolving Space Activities, Vol. 2, Article No. 165, 2024